



CENTRAL UNIVERSITY OF KARNATAKA

SCHOOL OF PHYSICAL SCIENCES

DEPARTMENT OF PHYSICS

TIME SERIES FORECASTING OF ACTIVE GALACTIC NUCLEI USING ARIMA MODEL

Project report submitted by

Jishnu Vijayan

2021

in partial fulfillment for the requirements of the degree of
Master of Science in Physics

Date of Submission: 06-06-2021

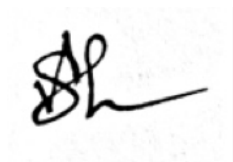
Supervised by: Dr. Amit Shukla

Declaration

This project work was done by Jishnu Vijayan bearing registration no. 2019MPH15 from Department of Physics, Central University of Karnataka under my guidance at Indian Institute of Technology Indore, Simrol 453552 from 02/02/2021 to 31/05/2021.

Name of Supervisor : Amit Shukla

Designation : Assistant Professor



Discipline of Astronomy, Astrophysics and Space
Engineering, Indian Institute of Technology Indore

Signature with Seal

In-house mentor : Dr. Deepak Samuel

Designation : Associate Professor
Department of Physics
Central University of Karnataka

Acknowledgements

This project was completed with the help of several people. I would like to express my sincere gratitude to all of them. First of all, I am extremely grateful to my project supervisor Dr. Amit Shukla for his valuable guidance, scholarly inputs and consistent encouragement I received throughout the work. I am deeply indebted to the Discipline of Astronomy, Astrophysics and Space Engineering Indian Institute of Technology (IIT) Indore for giving me an opportunity to work. I owe my deepest gratitude to Sushmita Agarwal and Pooja Tanty, for their valuable suggestions throughout this work. I sincerely acknowledge all my teachers from Department of Physics, Central University of Karnataka from whom I learnt the basics of Physics.

Abstract

Active galactic nuclei (AGNs) are significant centers of high-energy radiation. Accretion of matter into the supermassive black hole at the center of host galaxy is believed to be the origin of enormous emission. This emission scatter across the entire electromagnetic spectrum. Their arbitrary variability in TeV γ -rays is seen as key to extricate the intricacy of the various underlying processes. Since the first discovery in 1989, 200 supplementary origins of TeV γ -rays have been appended to the category of these cosmic accelerators. Blazars are one of the powerful sub-classes of active galactic nuclei. Long-term and regular observations of blazars are the key to obtain statistics on the interplay of the black holes, radio jets, and accretion disks.

The flux variability of two blazars, NGC 1275 and Markarian 421 is evaluated utilizing a time series analysis of the light curves acquired with the Fermi Gamma-ray Space Telescope and the First G-APD Cherenkov Telescope respectively. Gaps in light curve of Markarian 421 and future flux of NGC 1275 are forecasted using Auto Regressive Integrated Moving Average Model. This aid to understand how the source varies over time, in that way the duty cycle of the source.

Contents

List of Figures	6
1 Active Galactic Nuclei	1
1.0.1 The Grand Unified Theory	1
1.0.2 Blazar	4
1.0.3 Relativistic Beaming and Doppler Boost	4
1.0.4 Stimulation for Blazar Research	5
2 Detection of the Non-Thermal Radiation	6
2.0.1 Cherenkov Radiation	7
2.0.2 The First G-APD Cherenkov Telescope	8
2.0.3 Fermi Gamma-ray Space Telescope	9
3 Time Series Forecasting	11
3.0.1 ARIMA Model	11
4 Results	15
4.1 Time Series Analysis of NGC 1275 Data	15
4.1.1 Test for Stationarity	15
4.1.2 ADFT Test	16
4.1.3 Time Series Decomposition	17
4.1.4 Make Time Series Stationary	19

Contents	5
4.1.5 ARIMA Modelling	20
4.1.6 Observations	21
4.2 Markarian 421	23
4.2.1 Time Series Forecasting of Mrk 421	24
5 Conclusions	27

List of Figures

1.1	Structure of Active Galactic Nuclei	3
1.2	Radio emission classification of AGN	4
2.1	Detection of VHE γ -ray by IACT	7
2.2	The First G-APD Cherenkov Telescope	8
2.3	Structure and components of FGST	9
4.1	NGC 1275 Time Series	16
4.2	ADFT test Result	16
4.3	Autocorrelation plot	17
4.4	Partial Autocorrelation plot	17
4.5	Components of Time Series	18
4.6	Differenced time series of lag 1	19
4.7	Dickey fuller test result	19
4.8	ACF plot of transformed time series	20
4.9	PACF plot of transformed time series	20
4.10	Modelled time series and initial time series	21
4.11	ARIMA predicted time series for next 400 days	22
4.12	Lognormal fit of AGN data	22
4.13	Light curve of Mrk 421	24
4.14	ARIMA forecasted light curve of Mrk 421	25

4.15 Histogram of FACT data	26
4.16 Histogram of predicted flux and the FACT data.	26

Chapter 1

Active Galactic Nuclei

The central region of galaxy is called galactic nucleus. Majority of radiations coming from nucleus of a normal galaxy are in visible wavelength range and are thermal radiations. But certain galaxies emit enormous amount of radiation from their nuclear regions. These central regions of galaxies have much higher luminosity than the rest of the galaxies itself. Emissions from these nuclei spread across the entire electromagnetic spectrum. Such galactic nuclei are called active galactic nuclei (AGN). Galaxies hosting active nuclei are called active galaxies. Between 2% - 10% of discovered galaxies are active. The spectral emission distributions of radiations coming from these nuclei are characterized as non-thermal emissions and cannot be attributed to stars. Such excess non-stellar emission has been ascertained within the radio, microwave, infrared, optical, ultra-violet, X-ray and gamma ray wavebands. The emission of non-stellar radiation from an AGN is attributed to the accretion of matter by a supermassive black hole of mass $10^8 M_{\odot}$ - $10^{10} M_{\odot}$ at its center. Fluxes emitted by these AGNs vary over different time scales.

1.0.1 The Grand Unified Theory

The classification of AGN appears to be confusing because of the large diversity. Unified theory, one of the most accepted unification models of Active Galactic Nuclei is suggested by Urry and Padovani in 1995 [1]. According to this model, different classes of AGN are different manifestations of the same phenomena. Different inclinations of AGN to the line-of-sight to Earth result difference in observed emissions.

All AGNs seem to share some common properties despite of their large diversity. There is a supermassive black hole at the core of every AGN, with masses larger than $10^5 M_{\odot}$ and going up to billions of solar masses [2]. The Schwarzschild radius of the black holes is in the range of light-seconds to light days. The potential well of the black holes attracts matter and converts the potential energy of the surrounding medium into radiation, resulting the output of the AGN. Thus, measuring the luminosity of the AGN over all wavebands will give an estimate of mass of the black hole. A hot, rotating accretion disk of dust and gas, stabilized by the angular momentum of the attracted matter surrounds the black hole. It emits mainly optical, and ultraviolet light. Dimensions for the accretion disk are of sub-parsec order. An opaque structure of dust called central torus covers the accretion disk. Dimensions of the torus are in range from 0.1 parsec to 10 parsec. Its opening axis is called as the ionization cone. The dust in the torus absorb radiations emitted by accretion disk and re-emit them in infrared range.

Central black hole region of a radio-loud AGN has powerful jets. These jets of relativistic particles are oriented perpendicular to the accretion disk. They extend up to kilo parsec and mega parsec [3]. Highly collimated EM radiations emitted by these jets are mainly non-thermal synchrotron radiations. High energy radiations are also emitted by these jets via inverse Compton or some hadronic processes. Therefore, the frequency and power of jet photon measured from Earth are dependent on the orientation of jet with respect to the line-of-sight to Earth, in agreement with the unified theory of AGN.

The basic structure of AGN is shown in Figure 1.1. The black hole, accretion disk, and torus surrounding accretion disk are represented on the left. A region near the black hole called corona is a source of relativistic electrons. High energy radiations are emitted by inverse Compton scattering of these electrons with photons from accretion disk [4]. Magnetic fields which are produced by the accretion disk lead to the launch of two-sided jet. Photons of the in-homogeneous jet appear to be moving at superluminal speeds from the point of view on Earth. Broad line region clouds near the central region of the AGN are represented by small circles. These clouds absorb radiations from accretion disk and re-emit them. This result in broad emission lines in AGN spectrum. The low-density clouds further away from AGN are responsible for narrow emission lines in AGN spectrum [5]. The distance each cloud from the centre of supermassive black hole in units of the Schwarzschild radius are represented in logarithmic scale.

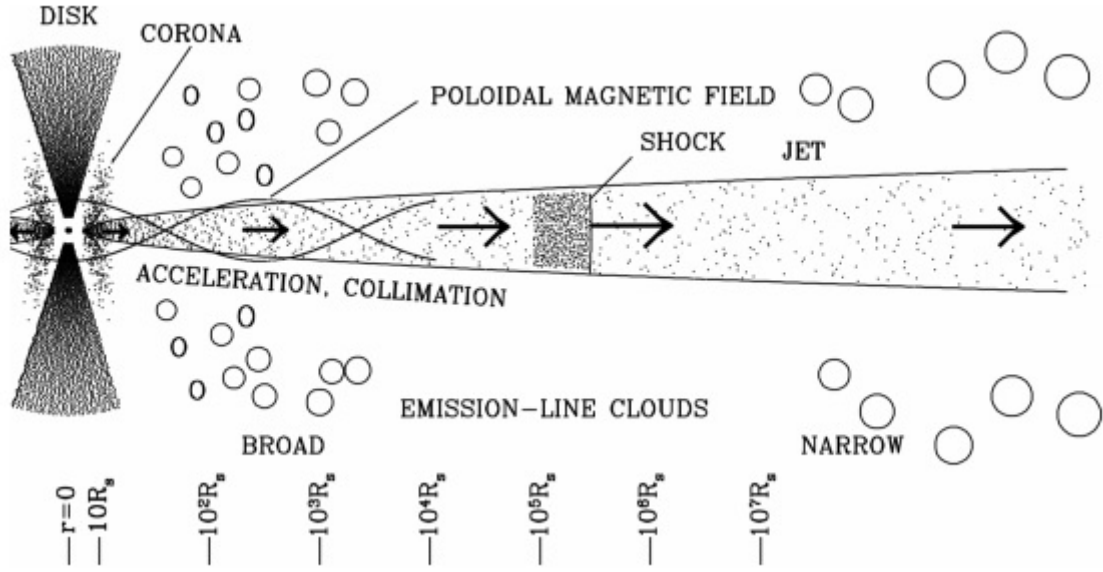


Figure 1.1 Structure of Active Galactic Nuclei

According to their radio emission, AGNs are also classified in two groups (i) radio loud and (ii) radio quiet. Depending on the optical spectral line widths, the Radio-quiet galaxies are further divided into Seyfert galaxies and Quasi Stellar Objects (QSO). Radio Galaxies and Blazars are sub-classes of radio-loud AGNs.

In the Urry and Padovani's model, AGNs are classified as Type I and Type II on the basis of spectral emission lines. An AGN having both broad emission lines (BEL) and narrow emission lines (NEL) in its spectrum is called Type I AGN. An AGN having only NEL in its spectrum is a Type II AGN. If an AGN is observed edge-on, the torus plane obscure radiations from broad line region clouds. Hence only NELs will be visible, and such an AGN appear as a Seyfert II (Sy II) galaxy in the case of radio quiet AGN, and narrow line region galaxy (NLRG) in case of radio loud AGN. But, if the observer's line of sight is close to the axis of the torus, both BELs and NELs are visible, and the AGN appears as a Seyfert I (Sy I) galaxy in the case of radio quiet AGN and broad line region galaxy (BLRG) in case of radio loud. If AGN is observed face-on to the jet, non-thermal, featureless continuum emission starts to dominate the entire source spectrum due to strong relativistic boosting effects. Blazars or a flat spectrum radio quasar (FSRQ) are observed in this orientation. Broad classification of AGN based on radio emission is represented in figure 1.2.

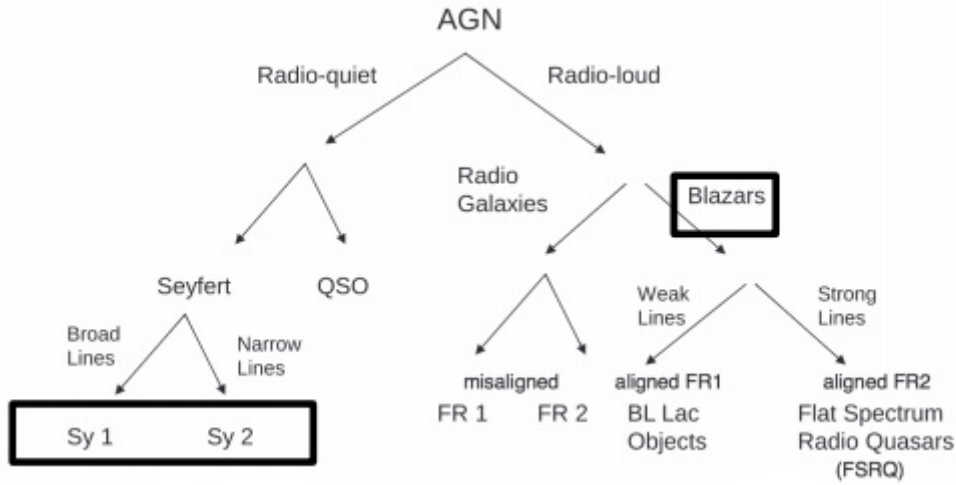


Figure 1.2 Radio emission classification of AGN

1.0.2 Blazar

A blazar is a radio-loud AGN with a relativistic jet directed towards the Earth (observer). Hence, spectrum of this powerful sub-class of AGN is dominated by featureless non-thermal continuum emission. Relativistic beaming and Doppler boosting of electromagnetic radiation from the jet categorizes blazar as the brightest AGN. The Blandford-Znajek process [6] explains how a spinning supermassive black hole twists its magnetic fields into coils. This motion creates a current of electrons and positrons that flow out from the black hole in both directions, accelerated by the twisting magnetic field. Superluminal motion of some blazar jets is yet another consequence of material in the jet traveling toward the observer at nearly the speed of light. BL Lac objects and optically violently variable (OVV) quasars are classifications of blazars. BL Lac objects are intrinsically low-power radio galaxies and OVV quasars are intrinsically powerful radio-loud quasars. Astronomer Edward Spiegel invented the name "blazar" in 1978 to denote these two classes.

1.0.3 Relativistic Beaming and Doppler Boost

The observed flux is Doppler boosted due to relativistic effects when a source emitting radiation moves with a relativistic velocity towards the observer. This effect is known as relativistic beaming. Doppler effect can increase the frequency of observed radiation.

1.0.4 Stimulation for Blazar Research

Blazars are special research topics in astronomy and high-energy astrophysics. As the non thermal radiations from jets of AGN are directed towards Earth, blazars are excellent sources to understand environment within the jets. Since high luminosity flux from blazar spread across the entire electromagnetic, multi wavelength flux and spectral studies gives different aspects of blazar. The uncertainty regarding jet composition still remains the same. It is unclear whether jets are composed of electron-proton pairs or electron positron pairs. Blazars exhibit rapid flux variability on multiple timescales. Origin of high variability of flux brightness, contents of blazar jets, role of magnetic fields in origin and propagation of relativistic jets and the dominant acceleration mechanism for the underlying radiating particles are still subjects of study.

Chapter 2

Detection of the Non-Thermal Radiation

The Earth's atmosphere act as a shield to Very high energy γ -rays. They are are completely absorbed at the atmosphere. Direct detection of these radiations by ground based telescopes is therefore not feasible. The ratio of VHE γ -ray to cosmic rays (CR) is about 10^{-4} for particles reaching Earth from the galactic plane and 10^{-5} for particles with extra galactic origin [7]. Space-based detectors have small collection areas about a few hundreds of square centimeters. Hence, such detectors are less effective in detecting high and very high energy (10 GeV - 100 TeV) γ -ray photons. The γ -rays produce showers of secondary particles at the top of Earth's atmosphere. Thus, the problem can be solved by detecting these showers using telescopes with large collection areas. This technique is called the Atmospheric Cherenkov Technique (ACT) [8][9].

Interaction of VHE γ -ray or cosmic ray with the air molecules at the top of the atmosphere produce showers of secondary particles. These showers are called as extensive air showers (EAS) and can be detected on the ground [10]. Very energetic secondary particles of these showers move at nearly the speed of light. These particles emit Cherenkov radiation if they move at a speed higher than the local speed of light in air.

2.0.1 Cherenkov Radiation

When a charged particle passes through a dielectric medium at a velocity greater than the speed of light in that medium, an electromagnetic radiation is emitted. This radiation is called Cherenkov radiation. This phenomenon was experimentally detected by Pavel Cherenkov in 1934 and a theoretical explanation of this effect was developed by Igor Tamm and Ilya Frank. The local electromagnetic field of the medium gets disturbed as the charged particle passes through it. It momentarily polarizes the medium by pushing like charges in the atom away, and inducing a dipole state. As the charge passes away, the dipole field in the dielectric collapses with the emission of Cherenkov radiation [11].

The Cherenkov light flash emitted by the air shower lasts for only nano-seconds and is hidden in a sea of night-sky background photons. These air showers have an ellipsoid like shape, which points back to the origin (incoming γ -rays or cosmic rays). The Cherenkov light produced by these EAS can be detected using an array of optical detectors having fast camera/photo-multiplier tubes (PMTs) at ground level. Technological advancement and dedicated efforts have given rise to a multitude of Imaging Air Cherenkov Telescopes (IACTs).

The figure 2.1 depicts a simple schematic representation of detection of VHE γ -rays by Cherenkov telescope.

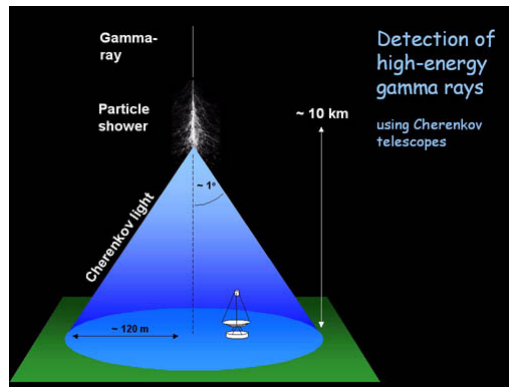


Figure 2.1 Detection of VHE γ -ray by IACT

2.0.2 The First G-APD Cherenkov Telescope

The First G-APD Cherenkov Telescope (FACT) is an IACT located at the Observatorio del Roque de los Muchachos, 2200 meters above sea level. It is designed to observe VHE γ -rays by measuring Cherenkov light. Image of FACT is shown in figure 2.2. The telescope's dish has a diameter of 3.8 meters and consists of 30 hexagonal mirrors. These mirrors reflect the incoming Cherenkov light into the telescope's camera. The camera has a total field-of-view (FoV) of 4.5° and consists of 1440 individual pixels fitted with a G-APD and a light concentrator each.



Figure 2.2 The First G-APD Cherenkov Telescope

Instead of photomultiplier tubes (PMTs), the FACT telescope camera uses silicon photomultipliers (SiPMs) for photo detection. It is the first Cherenkov telescope employing this new technology. Compared to PMTs, SiPMs need a much lower operation voltage, are more robust and have a higher photon detection efficiency. Consequently, these devices are promising for an IACT to improve the sensitivity of the instrument compared to PMTs. These SiPMs are made up of arrays of Geiger-mode avalanche photo-diodes (G-APDs). FACT is a pathfinder telescope to explore the long-term operation of SiPMs in Cherenkov astronomy. SiPMs allow for observations during bright nights, including during full Moon, which provides large duty time by

reducing the amount of gaps in the observation schedule and increases the telescope's up-time.

The FACT will observe extra-galactic objects as it is situated on northern hemisphere. Long-term monitoring of bright AGNs to spot bright flares, observe their time behavior effectively, correlate them with signals obtained at lower energies (X-ray, optical, radio) or even with these of neutrino detectors and to study the statistics and the types of the flares are the fundamental objectives of FACT.

2.0.3 Fermi Gamma-ray Space Telescope

Fermi Gamma-ray Space Telescope (FGST) is a telescope which is being used gamma-ray astronomy. It is space based low Earth orbit telescope. Fermi follows a circular orbit around Earth at an altitude of 550 km and at an inclination of 28.5 degrees. On 2008 June 11, the Delta II Heavy launch vehicle launched by NASA carried the telescope to the Earth orbit. An artistic rendition of FGST is shown in figure 2.3.

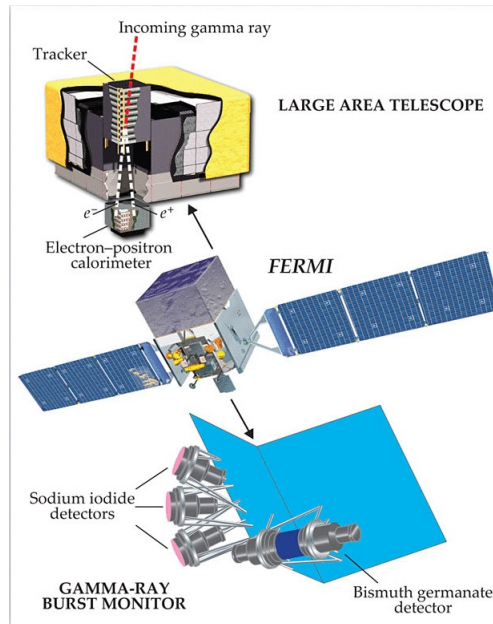


Figure 2.3 Structure and components of FGST

There are mainly two scientific equipment in FGST, the Large Area Telescope (LAT) [12] and the Gamma-ray Burst Monitor (GBM) [13]. LAT is an imaging gamma-ray detector. It covers 20% of the sky at any given moment and covers the entire sky every 3 hours. It is a high-energy γ -ray telescope, covering the energy range from 20

MeV to more than 300 GeV. The LAT is an output of an international collaboration of high-energy particle physics institutes, space agencies and universities in France, Japan, Sweden, Italy and the United States. Since γ -rays cannot be focused, the LAT is instrumented to detect the track trajectory of the electrons and positrons that are produced when an incident γ -ray undergoes pair-conversion in a thin, high-Z foil. It measures the energy of the resultant electromagnetic shower that develops in the telescope's calorimeter. The GBM consist of 14 scintillation detectors. It can detect γ -ray bursts at photon energies from 8 KeV to 40 MeV across the whole sky not obstructed by the Earth.

Some of the main scientific objectives of Fermi mission include (1) Studying the physics of γ -ray bursts, (2) Understanding the particle acceleration mechanisms operating in celestial sources, particularly in AGNs, pulsars, supernovae remnants, and the Sun. (3) Studying energy spectra and cause of wavelengths variability of light coming from blazars so as to determine the composition of the black hole jets aimed directly at Earth and so on.

Chapter 3

Time Series Forecasting

A sequence of observations recorded at regular time intervals is known as time series. A time series may be hourly, daily, weekly, monthly and annually, depending on the frequency of observations. Time-series analysis is a mandatory tool in astronomy and astrophysics. Astronomers observe the light arriving from distant objects at equal time intervals and look for repeating patterns, develop theories through inductive reasoning. Time series analysis involves understanding various aspects about the inherent nature of the series so that an accurate forecast can be made. This chapter focuses on a special type of forecasting method called ARIMA modeling. In this thesis, the amount of flux emitted over equal intervals of time from blazars, NGC 1275 and Markarian 421 are searched for repeating patterns and future flux are forecasted using ARIMA model.

3.0.1 ARIMA Model

ARIMA stands for ‘Auto Regressive Integrated Moving Average’. ARIMA is a model that explains a given time series based on its own past values, that is, its own lags and the lagged forecast errors, so that equation can be used to forecast future values. This model was created in 1970 by Gwilym, M.Jenkins and George E.P Box. ARIMA can capture complex relationships as it takes error terms and observations of lagged terms. ARIMA model is a combination of Auto Regressive model (AR) and Moving Average model (MA).

Auto Regressive Model (AR)

A pure Auto Regressive model is one where current value Y_t depends only on its own past values. That is, Y_t is a function of the lags of Y_t . AR model is characterized by parameter p . p is called order of AR term. p -th order AR term, $AR(p)$ has the general form

$$Y_t = \phi_0 + \phi_1 Y_{t-1} + \phi_2 Y_{t-2} + \cdots + \phi_p Y_{t-p} + \epsilon_t \quad (3.1)$$

where

Y_t = Response (dependent) variable at time t .

$Y_{t-1}, Y_{t-2}, \dots, Y_{t-p}$ = Response variable at time lags $t-1, t-2, \dots, t-p$ respectively.

$\phi_0, \phi_1, \phi_2, \dots, \phi_p$ = Coefficients to be estimated.

ϵ_t = Error term at time t .

Moving Average Model (MA)

A pure Moving Average model is one where Y_t depends only on the lagged forecast errors. MA model is characterized by parameter q . q is called order of MA term. q -th order MA term, $MA(q)$ has the general form

$$Y_t = \mu + \epsilon_t - \theta_1 \epsilon_{t-1} - \theta_2 \epsilon_{t-2} + \cdots - \theta_q \epsilon_{t-q} \quad (3.2)$$

where Y_t = Response (dependent) variable at time t .

μ = Constant mean of the process.

$\theta_1, \theta_2, \dots, \theta_q$ = Coefficients to be estimated.

ϵ_t = Error term at time t .

$\epsilon_{t-1}, \epsilon_{t-2}, \dots, \epsilon_{t-q}$ = Errors in previous time periods that are incorporated in the response Y_t .

Differencing

A non-stationary time series can be made stationary by various methods. One such method is "differencing". That is, subtract the previous value from the current value.

Sometimes, depending on the complexity of the series, more than one differencing may be needed. d is called the order of differencing. The value of d , therefore, is the minimum number of differencing needed to make the series stationary. And if the time series is already stationary, then $d = 0$. A time series made stationary after differencing once will have $d = 1$. A time series made stationary after differencing d times is represented as $I(d)$, where 'I' stands for 'Integrated'.

Thus ARIMA model is characterized by 3 terms: p, q, d

where,

p is the order of the AR term.

q is the order of the MA term.

d is the number of differencing required to make the time series stationary.

ARIMA(p, d, q) has the general form,

$$Y_t = \phi_0 + \phi_1 Y_{t-1} + \phi_2 Y_{t-2} + \cdots + \phi_p Y_{t-p} + \epsilon_t - \theta_1 \epsilon_{t-1} - \theta_2 \epsilon_{t-2} + \cdots - \theta_q \epsilon_{t-q} \quad (3.3)$$

We can use the autocorrelation function (ACF) and the partial autocorrelation function (PACF) plots of sample to determine the parameters of ARIMA model.

Standard procedure for ARIMA Modelling

Standard procedure followed for time series forecasting using ARIMA MODEL:

1. Plot the Time series.
2. Transform time series to a stationary time series.
3. Splitting Original time series into different components
 - Trend.
 - Seasonality.
 - Irregularity (Check for correlation in the residual component).
4. Check for stationarity of time series. If it is not stationary, making it stationarity by applying transformation on data as ARIMA model works on assumption that time series is stationary. Conducting the test for Stationarity.

- **Visual Test (Rolling Statistics Test).**

Plotting moving average and moving standard deviation and checking if it varies with time.

- **Augmented Dickey-Fuller Test (ADCF Test).**

Null hypothesis is that time series is non- stationary. Test results consist of test statistics and some critical value.

If Test statistics < Critical Value, we reject null hypothesis – Series is stationary.

- **PACF plots and ACF plots.**

If ACF plots decays slowly, PACF decays relatively quickly – Time series is non - stationary. If PACF and ACF decays quickly, time series is stationary.

5. Find the p,d,q parameters for ARIMA (p,d,q) modelling:
6. Plotting ACF AND PACF plots to know the value of p and q. If n-order differencing is need to make data stationary, then $d = n$.
7. ARIMA modelling on our time series followed by forecasting the future values.

Chapter 4

Results

In this project, the time series of flux from NGC 1275 observed by Fermi Gamma-ray Space Telescope at different time has been provided. The time is in Mean Julian Days (MJD). The data provided has a 10 days difference till MJD 58187.6500347222 after which there is a data gap of 43 days. The data has been rejected after 58187.6500347222 due to this redundancy. NGC 1275 is an elliptical galaxy located about 250 million light-years away in the constellation Perseus. It was discovered by astronomer Heinrich d'Arrest on February 14, 1863 [14]. NGC 1275 has a supermassive black of mass $6 \times 10^9 M_{\odot}$ at its centre [15]. Because of its emission-line optical spectrum where broad lines are detected, NGC 1275 has been variously classified as a Seyfert 1.5. Due to the strong and rapid variability of the continuum emission and its polarization, its is also considered as a blazar. In the radio, NGC 1275 hosts the exceptionally bright radio source Perseus A, also known as 3C 84. The source 3C 84 has a strong and compact nucleus [16].

4.1 Time Series Analysis of NGC 1275 Data

4.1.1 Test for Stationarity

Visual Test

On plotting the Flux variation with time and the corresponding Moving Average (indicated by red line) and Moving Standard Deviation (indicated by blue line) over a

9 years (350 data points) window, an upward trend is visible. Also see the standard deviation increasing with time. Hence Time Series is not stationary.

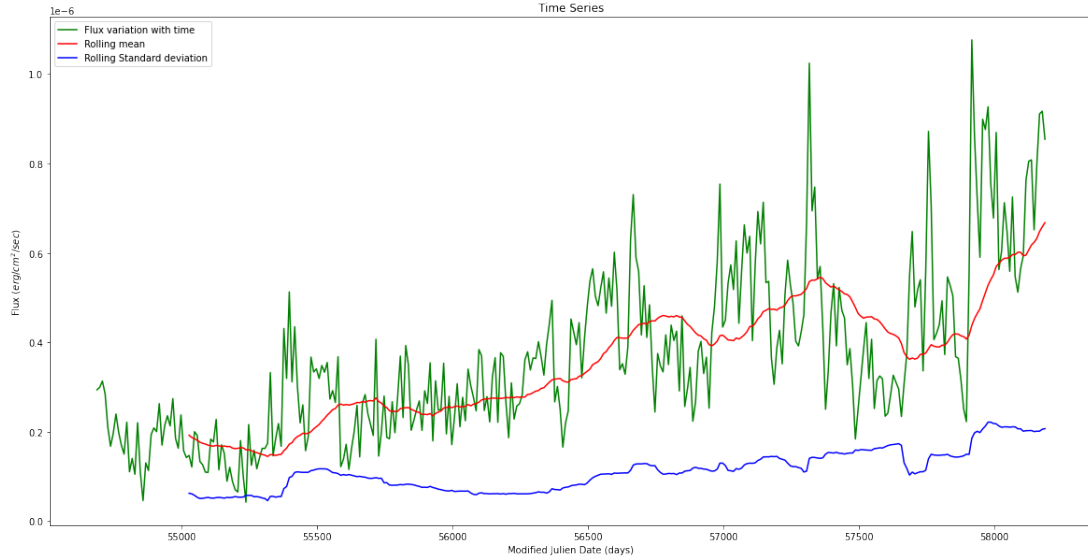


Figure 4.1 NGC 1275 Time Series

4.1.2 ADFT Test

Dickey fuller test for the given time series points at the non-stationarity of data.

p value = 0.805 > 0.05 Hence, non stationary.

Also, Test Statistics > Critical Value → non stationary.

```
Weak evidence against null hypothesis, time series has a unit root . Indicating it is NOT STATIONARY
test statistics          -0.846661
p-value                 0.805030
#Lags Used              16.000000
Number of Observations Used  334.000000
Critical value(1%)       -3.450081
Critical value(5%)       -2.870233
Critical value(10%)      -2.571401
dtype: float64
```

Figure 4.2 ADFT test Result

PACF and ACF Plots

On plotting the PACF plot and ACF plot, it is seen that:

- ACF is decaying exponentially.

- PACF decays immediately and a strong correlation is observed for lag 1.
- Correlation for other lags is found to have values which are statistically very low (within the blue limit).

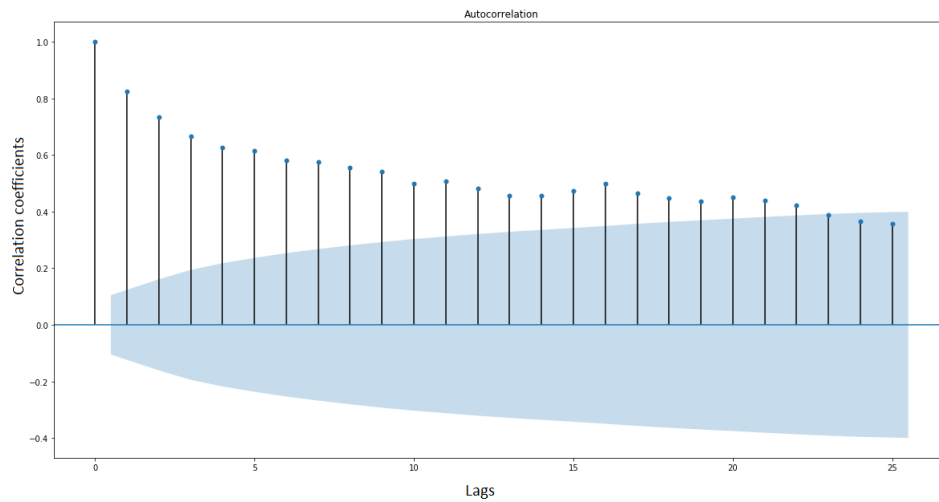


Figure 4.3 Autocorrelation plot

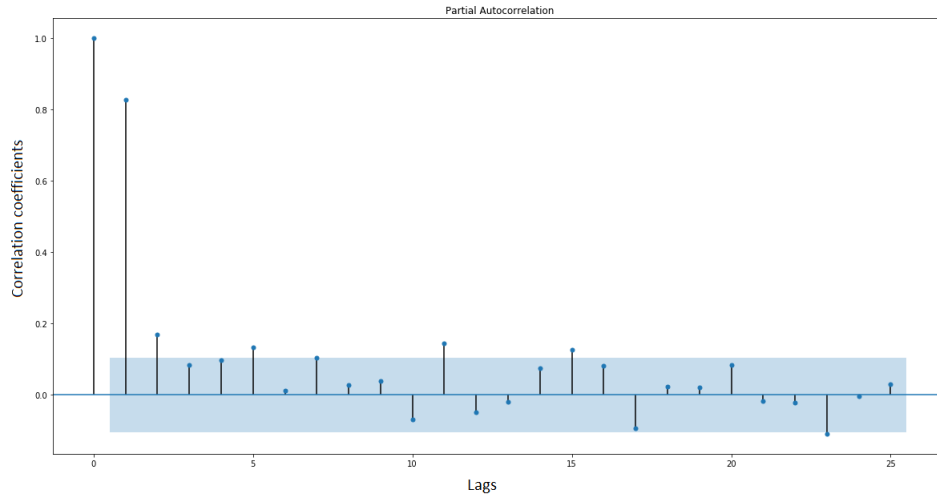


Figure 4.4 Partial Autocorrelation plot

4.1.3 Time Series Decomposition

If we use the additive model to decompose our time series:

$$\text{Original}(t) = \text{Trend}(t) + \text{Seasonal}(t) + \text{Residual}(t)$$

Considering each of these component are independent of one another, the decomposed data shows a clear upward trend, seasonality component and residual part.

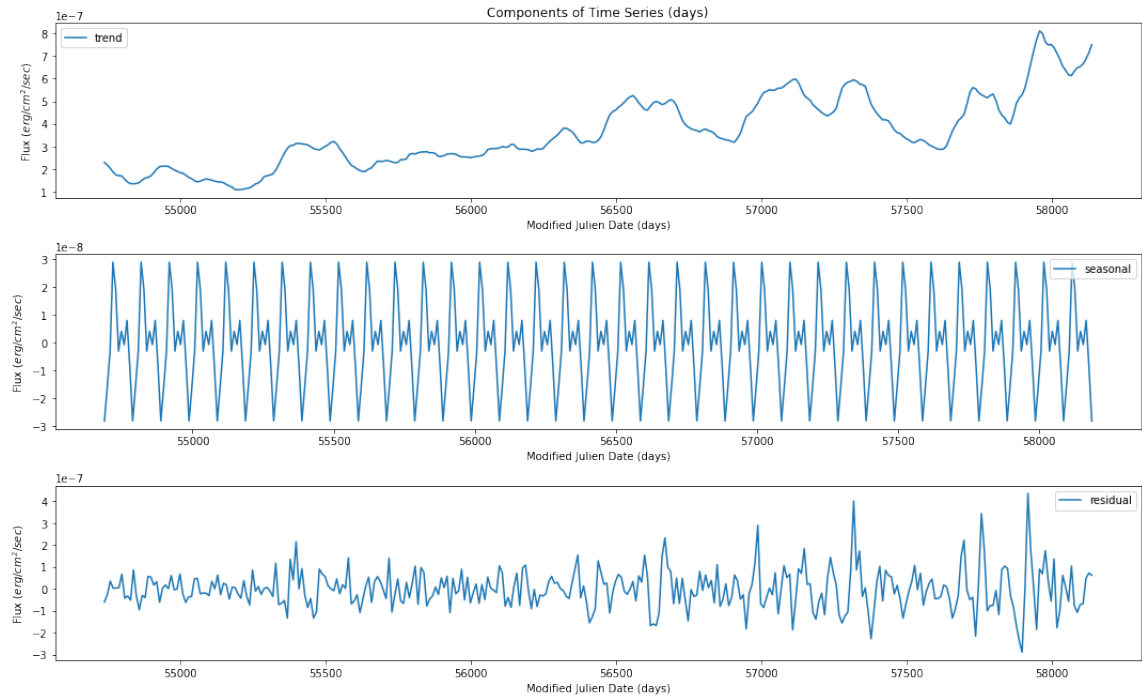


Figure 4.5 Components of Time Series

4.1.4 Make Time Series Stationary

On carrying a 1-lag difference, time series became stationary. Plot of transformed time series is shown in figure 4.6. The visual test gives a clear check on stationarity. The mean and standard deviation are sufficiently constant over the entire time.

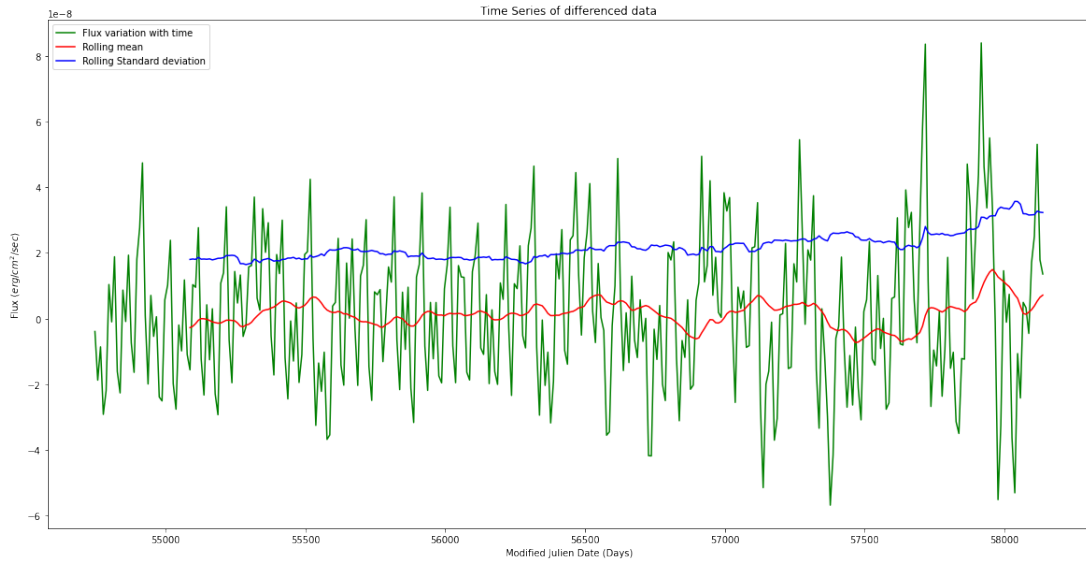


Figure 4.6 Differenced time series of lag 1

```
Strong evidence against null hypothesis, reject the null hypothesis. Data has no unit root and is STATIONARY
test statistics      -6.232511e+00
p-value             4.914246e-08
#Lags Used          1.500000e+01
Number of Observations Used  3.240000e+02
Critical value(1%)    -3.450695e+00
Critical value(5%)    -2.870502e+00
Critical value(10%)   -2.571545e+00
dtype: float64
```

Figure 4.7 Dickey fuller test result

On checking stationarity through the ADFT, it is found that p value is very small. Also,

Test Statistics < Critical Value.

Thus, 1 lag differenced data is stationary.

4.1.5 ARIMA Modelling

Determining parameters p, d and q

Since a 1 lag difference of data is Stationary, $d = 1$. The differenced time series is 'de-noised' by removing residual part. p and q are found from PACF and ACF plots respectively of transformed time series. ACF plots decays off and enters the statistical zero region when lag = 2. This gives possible q value that can be used for modelling.

For both ACF and PACF, the exponential cutoff drops off to zero when lag = 2.

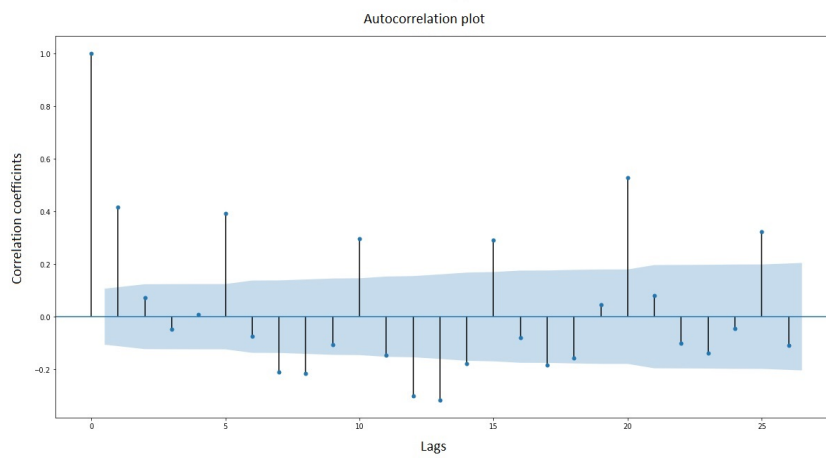


Figure 4.8 ACF plot of transformed time series

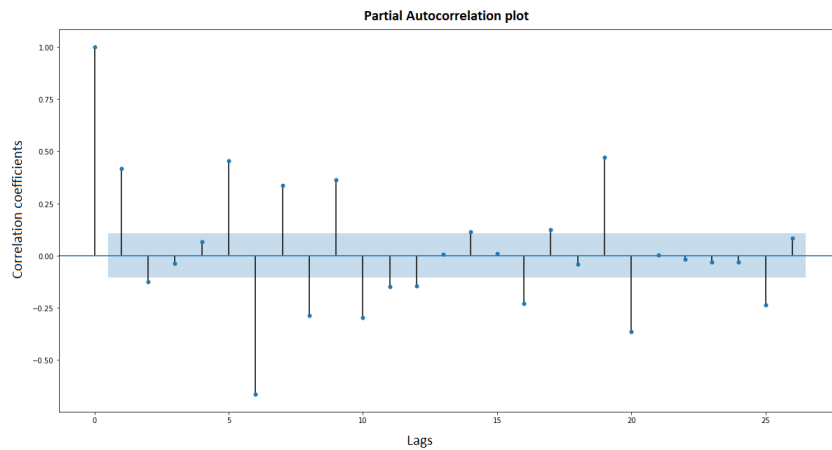


Figure 4.9 PACF plot of transformed time series

Therefore $p = 2$, $q = 2$ and $d = 1$ for ARIMA model.

4.1.6 Observations

A plot of modelled time series and initial time series (TS) (figure 4.10) shows that the ARIMA modelled time series is predicting slightly higher values than the actual Flux.

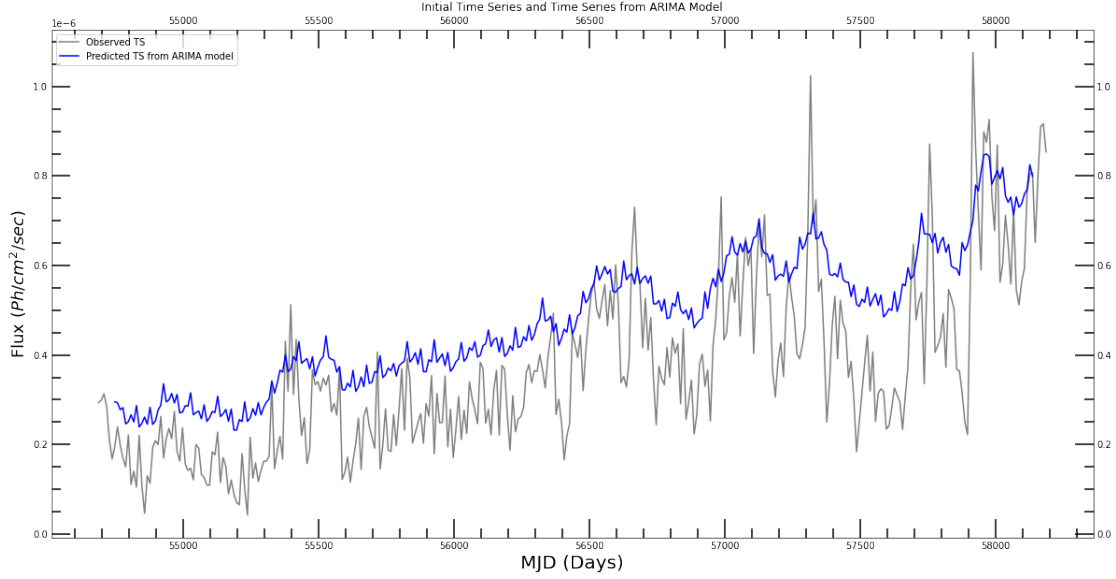


Figure 4.10 Modelled time series and initial time series

The modelled time series follows the trend and general pattern of the initial time series. Also, it is not able to work well for sudden dips in flux. Hence missing out on Seasonality component. A better choice of parameters might help to improve the fit.

The predictions from the above model for next 400 days (40 data points at a gap of 10 days) as forecasted by ARIMA model are:

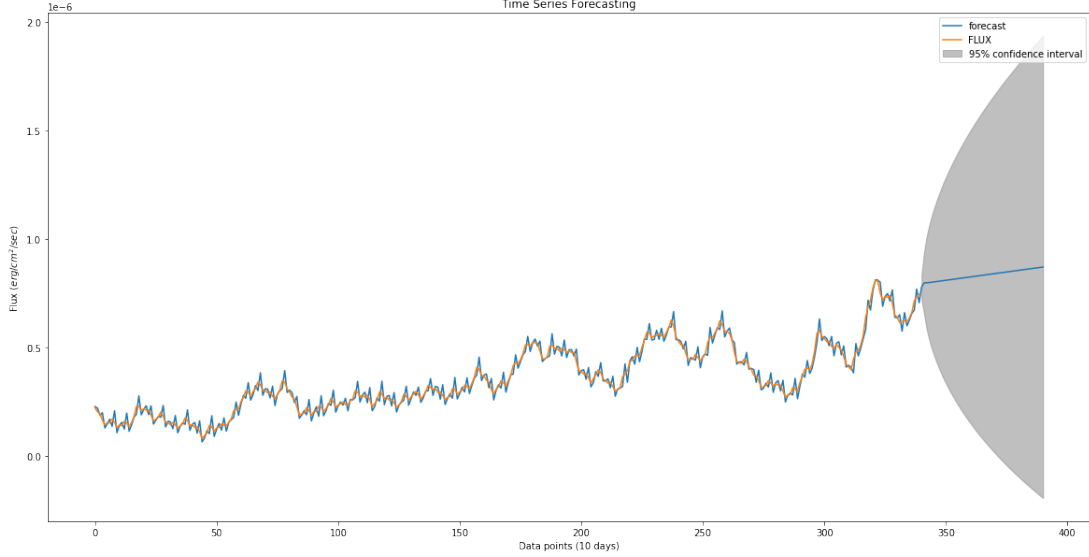


Figure 4.11 ARIMA predicted time series for next 400 days

The randomness of the noise component might pose as a major problem in prediction of flux. The flux values on itself have an error bar which can be a major problem for flux prediction from AGN. Improvement of choice of parameters (p , d , q) might further improve the results. From figure 4.12 it is clear that the histogram plot of AGN data fit to a log-normal function.

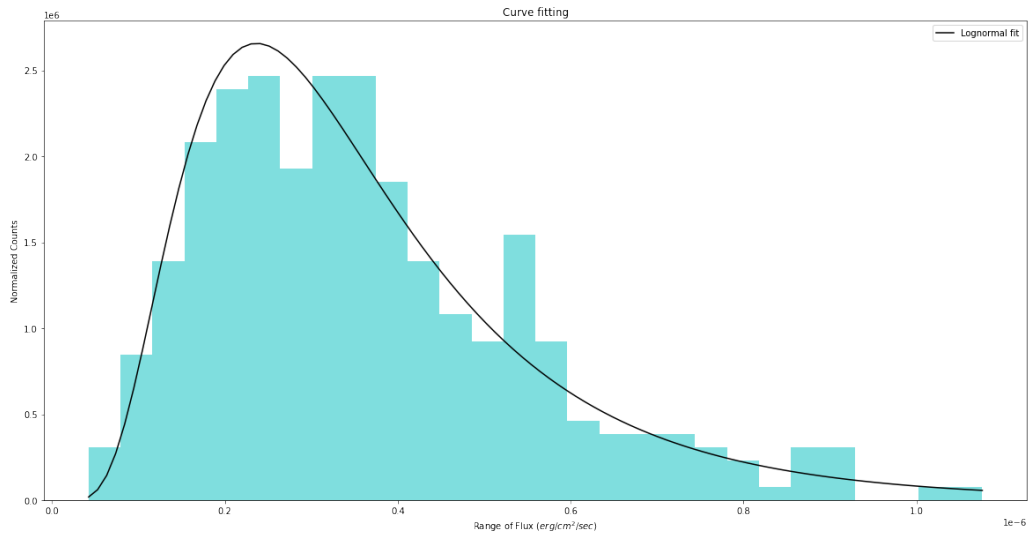


Figure 4.12 Lognormal fit of AGN data

4.2 Markarian 421

Markarian 421 (Mrk 421) the first discovered TeV blazar is located at distance about 397 million light-years from the Earth in the constellation Ursa Major. It is a BL Lacertae object, a subclass of AGN and also a strong source of γ -ray. It is one of the closest blazars to Earth, nominating it one of the brightest quasars in the night sky. It is still one of the few blazars that can be detected at TeV energies nearly all the time with ground-based imaging atmospheric Cherenkov telescopes.

It was first confirmed as a very high energy gamma ray emitter in 1992 by M. Punch at the Whipple Observatory [17]. Mrk 421 is a very active blazar with major outbursts about once every two years in γ -ray band [18]. A major outburst accompanied by many rapid flares usually lasts several months and with timescales from tens of minutes to several days. A profoundly brisk outburst in very-high-energy γ -ray was identified in 1996 by J. Gaidos at Whipple Observatory [19]. Markarian 421 also had an outburst in 2001 and is monitored by the Whole Earth Blazar Telescope Project [20].

4.2.1 Time Series Forecasting of Mrk 421

In this project, the light curve from Mrk 421 observed by the First G-APD Cherenkov Telescope (FACT) at different time has been provided. The time is in Modified Julian Days. The FACT provides data in the very high energy (VHE) range. FACT monitors the brightest TeV sources in the sky. The light curve of Mrk 421 along with error bars is shown in figure 4.13

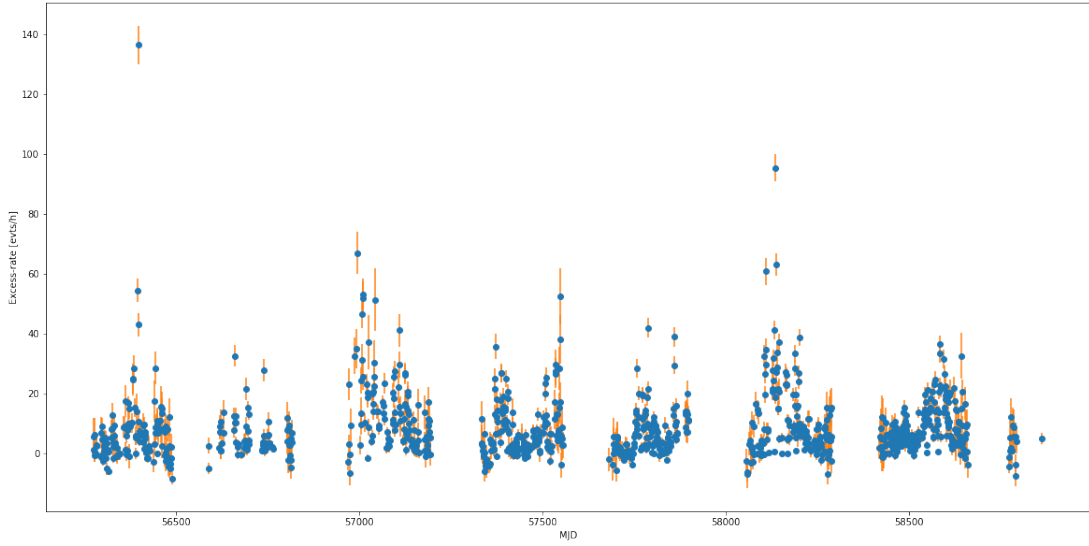


Figure 4.13 Light curve of Mrk 421

The sources are not visible 24 h per day since it is a ground based instrument. This causes gaps in the light curve. Seasonal gaps are introduced to the light curves as the observations are limited to night time. FACT telescope cannot operate during full moon days. Additional small gaps are caused by technical issues, bad weather and other environmental influences [21]. We tried to predict these gaps in light curve using ARIMA model. In addition, the plot clearly depicts high flux variability of Mrk 421. It remains in peak activity stage for very short time interval.

Time series analysis was done on the light curve. Seasonal gaps, small gaps to due bad weather and other technical issues were forecasted using ARIMA model. Thus the light curve became continuous. Forecasted light curve of Mrk 421 is shown in figure 4.14.

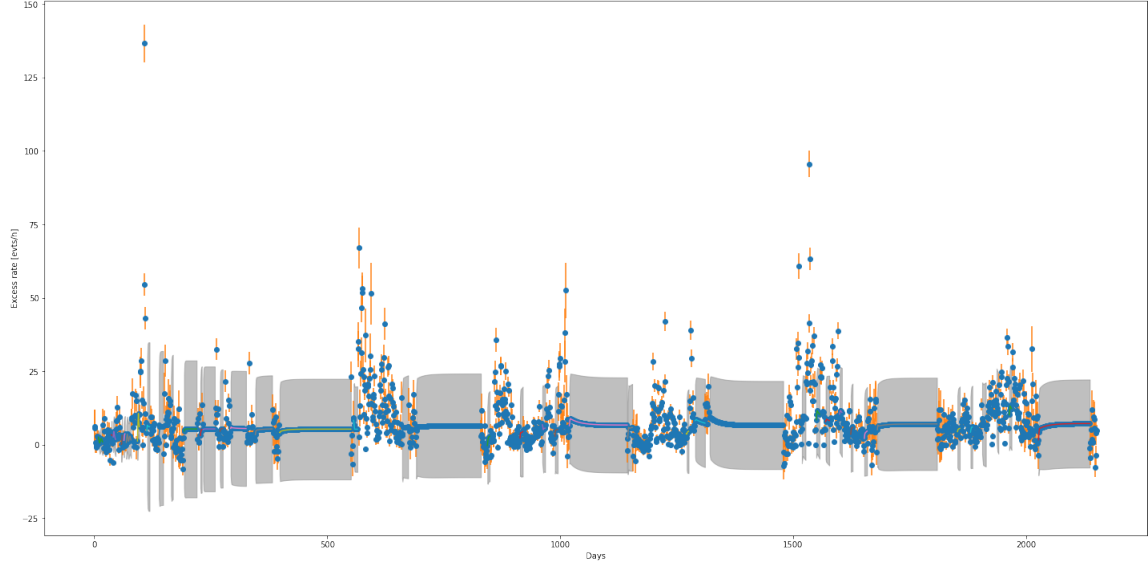


Figure 4.14 ARIMA forecasted light curve of Mrk 421

ARIMA understand that the overall predicted fluxes are more or less constants. But they can vary within the 95% confidence intervals (gray portions).

A histogram plot of FACT data can be used to represent the bins where predicted fluxes could come. It is shown in figure 4.15. Majority of ARIMA predicted fluxes are in range 5 (evts/h) - 8 (evts/h) fall into bins 10,11 and 12 marked red. Histogram of the FACT data and the ARIMA predicted values for gaps are shown in figure 4.16. Blue bins corresponds to FACT data and the red bins corresponds to ARIMA predicted values. It gives the number of times the predicted fluxes have occurred in a given flux range.

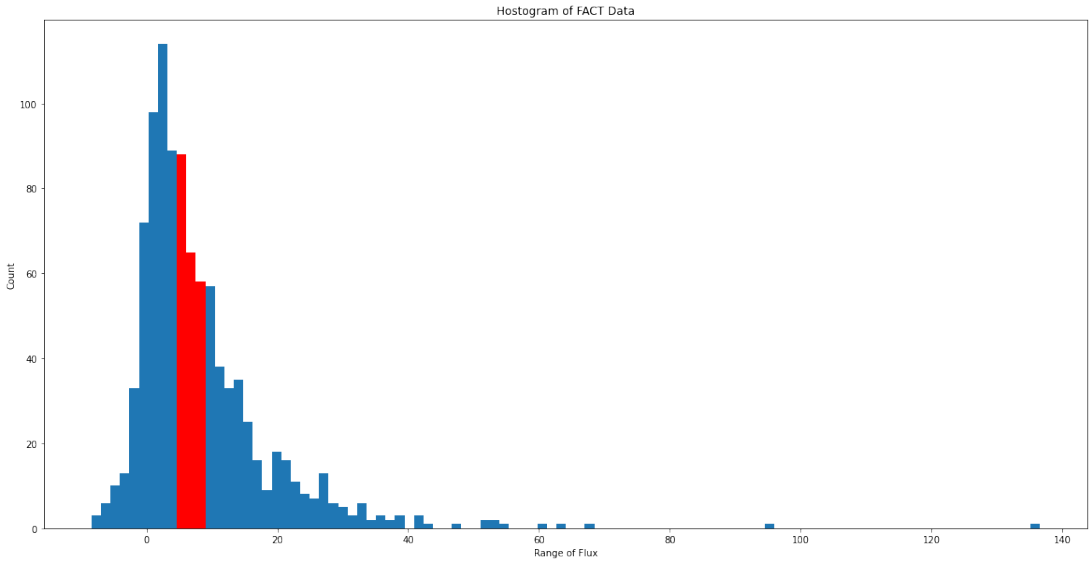


Figure 4.15 Histogram of FACT data

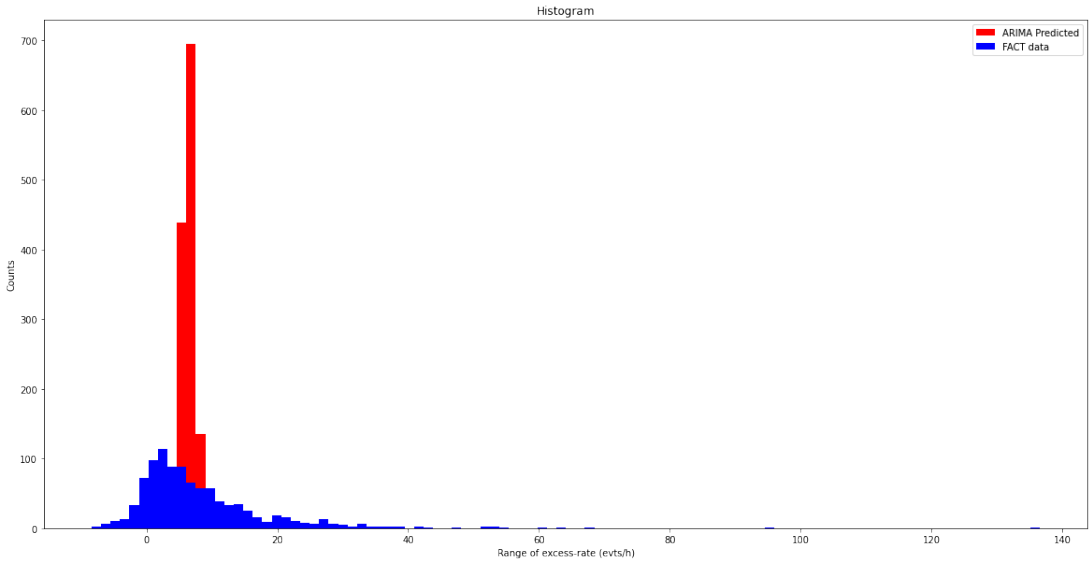


Figure 4.16 Histogram of predicted flux and the FACT data.

Chapter 5

Conclusions

Active galactic nuclei (AGNs) are significant centers of high-energy radiation. Accretion of matter into the supermassive black hole at the center of host galaxy is believed to be the origin of enormous emission. Their arbitrary variability in TeV γ -rays is seen as key to extricate the intricacy of the various underlying processes. Long-term and regular observations are the key to obtain statistics on the their underlying processes.

In this project, the time series of flux from NGC 1275 observed by Fermi Gamma-ray Space Telescope and Markarian 421 observed by FACT telescope respectively at different time were constructed. Different components of the time series were precisely identified. Various aspects about the inherent nature of both series were studied. The randomness of the noise component is a serous threat for flux prediction. The flux values on itself have an error bar which can be a major problem for flux prediction from AGN. Within the limitations of ARIMA model, future flux values of both sources were predicted. Time series forecasting furnish details about flux variability of the source. This aid to understand how the source varies over time, in that way duty cycle of the source.

Reference

- [1] C Megan Urry and Paolo Padovani. “Unified schemes for radio-loud active galactic nuclei”. In: Publications of the Astronomical Society of the Pacific 107.715 (1995), p. 803.
- [2] Frank M Rieger and K Mannheim. “On the central black hole mass in Mkn 501”. In: Astronomy & Astrophysics 397.1 (2003), pp. 121–125.
- [3] Michael Catanese and Trevor C Weekes. “Very High Energy Gamma-Ray Astronomy”. In: Publications of the Astronomical Society of the Pacific 111.764 (1999), p. 1193.
- [4] Alan P Marscher. “Relativistic jets in active galactic nuclei”. In: AIP Conference Proceedings. Vol. 856. 1. American Institute of Physics. 2006, pp. 1–22.
- [5] Hagai Netzer. “Revisiting the unified model of active galactic nuclei”. In: Annual Review of Astronomy and Space Physics 53 (2015), pp. 365–408.
- [6] Roger D Blandford and Roman L Znajek. “Electromagnetic extraction of energy from Kerr black holes”. In: Monthly Notices of the Royal Astronomical Society 179.3 (1977), pp. 433–456.
- [7] Mathieu de Naurois and Daniel Mazin. “Ground-based detectors in very-high-energy gamma-ray astronomy”. In: Comptes Rendus Physique 16.6-7 (2015), pp. 610–627.
- [8] Forrest I Boley. “Atmospheric Čerenkov Radiation from Cosmic-Ray Air Showers”. In: Reviews of Modern Physics 36.3 (1964), p. 792.
- [9] W Galbraith and JV Jelley. “Light pulses from the night sky associated with cosmic rays”. In: Nature 171.4347 (1953), pp. 349–350.
- [10] G Rowell et al. “A search for gamma rays above 0.5 TeV from the southern radio pulsar PSR1706-44”. In: (1998).

- [11] Boris M Bolotovskii. “Vavilov–Cherenkov radiation: its discovery and application”. In: Physics-Uspekhi 52.11 (2009), p. 1099.
- [12] WB Atwood et al. “The large area telescope on the Fermi gamma-ray space telescope mission”. In: The Astrophysical Journal 697.2 (2009), p. 1071.
- [13] M Ackermann et al. “Fermi-LAT observations of the gamma-ray burst GRB 130427A”. In: Science 343.6166 (2014), pp. 42–47.
- [14] Jenny E Greene et al. “The Stellar halos of massive elliptical galaxies. II. Detailed abundance ratios at large radius”. In: The Astrophysical Journal 776.2 (2013), p. 64.
- [15] N Arakawa, AC Fabian, and SA Walker. “The X-ray coronae of two massive galaxies in the core of the perseus cluster”. In: Monthly Notices of the Royal Astronomical Society 488.1 (2019), pp. 894–901.
- [16] Aous A Abdo et al. “Fermi discovery of gamma-ray emission from NGC 1275”. In: The Astrophysical Journal 699.1 (2009), p. 31.
- [17] Michael Punch et al. “Detection of TeV photons from the active galaxy Markarian 421”. In: nature 358.6386 (1992), pp. 477–478.
- [18] M Tluczykont et al. “Long-term lightcurves from combined unified very high energy γ -ray data”. In: Astronomy & Astrophysics 524 (2010), A48.
- [19] A Michael Hillas. “Cerenkov light images of EAS produced by primary gamma”. In: 19th International Cosmic Ray Conference (ICRC19), Volume 3. Vol. 3. 1985.
- [20] A Sillanpää, LO Takalo, Webt Collaboration, et al. “Optical monitoring of the blazar Mk421 during the TeV outburst”. In: International Cosmic Ray Conference. Vol. 7. 2001, p. 2699.
- [21] H Anderhub et al. “Design and operation of FACT—the first G-APD Cherenkov telescope”. In: Journal of Instrumentation 8.06 (2013), P06008.